Geochemical volcano monitoring

Alessandro Aiuppa[1], Mariano Agusto[2], Patrick Allard[3], Simon Carn[4], Maarten J. de Moor[5], Salvatore Inguaggiato[6], Agnes Mazot[7], Y. Moussallam[8], and Patricia Nadeau[9]

[1]Dipartimento di Scienze della Terra e del Mare, Università di Palermo, Palermo, Italy
[2]Universidad de Buenos Aires (UBA), National Scientific and Technical Research Council (CONICET), Buenos Aires, Argentina
[3]Institute de Physique du Globe (IPGP), Paris, France
[4]Geological and Mining Engineering and Sciences, Michigan Technological University, USA
[5]OVSICORI, Universidad Nacional, Costa Rica
[6]Istituto Nazionale di Geofisica e Vulcanologia, Sezione di Palermo, Palermo, Italy
[7]GNS Science, New Zeeland
[8]Lamont-Doherty Earth Observatory, Columbia University, New York, USA
[9]USGS Hawaiian Volcano Observatory, Hilo, USA

This is a peer-reviewed preprint submitted to EarthArXiv. The manuscript is part of Chapter 2.4 of The Encyclopedia of Volcanoes, 3rd ed. Editors: C. Bonadonna, L. Caricchi, A. Clarke, P. Cole, J. Lindsay, J. Lowenstern, R. Robertson and M. L. Villegas

Abstract - *The geochemistry of volcanic fluids is increasingly employed at volcano observatories worldwide to assess volcano activity state, and eruption potential. Here, we review the state-of-the-art in the field, with a primary focus on the most recent developments in instrumental gas monitoring that have rendered geochemistry an increasingly effective eruption-forecasting tool. We describe the main geochemical techniques, from both ground and space, and how they each contribute to volcano monitoring. By presenting some selected case studies, we demonstrate that geochemical monitoring strategies need to adapt as volcanic activity state evolves during unrest and in the run-up to eruption. Modern gas-monitoring networks need to integrate different instrumental tools and require collection of a variety of gas-related signals if any subtle change in volcano behavior is to be captured in a timely manner.*

Keywords: *fluid geochemistry; geochemical monitoring; volcanic gases; magmatic degassing; magmatic gas-hydrothermal interactions; direct sampling; remote sensing; volcanic plumes; soil degassing; crater lakes.*

1. Introduction.

Volcanoes emit magma-sourced volatiles through a variety of fluid manifestations, ranging from (i) large atmospheric plumes released by open-vent volcanoes to (ii) fumaroles, steaming grounds/mud pools, hot/cold spring waters, and degassing soils that represent the dominant emission forms at closed-vent, dormant volcanoes [1]. Geochemical monitoring is useful because volcanic fluids exhibit temporal changes in chemistry and mass flux that reflect critical changes in the magma and its surroundings, providing insights into the volcano and its potential for eruption.

The chemistry of volcanic fluids has now been investigated for more than a century, initially instigated by the curiosity of key volcano chemist pioneers [2]. However, it was not until the 1970s that geochemical observations became systematic enough to emerge as a potential tool for volcanic eruption forecasting [3]. It is today universally accepted that, in addition to contributing to volcano monitoring, fluid geochemistry is central to understanding magma degassing processes [4], the architecture of magma feeding systems [4, **add QR to Further Readings**], and estimation of the T-P-X conditions of volcano-hosted hydrothermal systems and their interactions with magmatic fluids [5]. Modern fluid geochemistry also contributes to sustainable development by offering a relatively inexpensive volcano monitoring tool, even in countries where volcanology is a still emerging field. Installation/maintenance of geochemical instrumentation remains an issue, however, especially for volcano observatories monitoring remote, poorly accessible volcanoes.

Broadly speaking, geochemical monitoring requires time series to be acquired for the composition and/or the flux (ideally both) of volcanic fluids. With a robust dataset in hands, and in combination with evidence streaming from other disciplines, geochemists interpret observed geochemical changes in reference to a conceptual model of volcano behavior (Fig. 1), from which they attempt to resolve any sign of volcano unrest or potential eruption.

Geochemical observations can be obtained via either (i) periodic surveys involving direct sampling or in-situ field measurement of fluids [3] or (ii) near-continuous records from fully automated field-deployed instruments [6-8]. Although the two strategies are very complementary, the second is intrinsically more beneficial for capturing the rapidly evolving dynamics of soon-to-erupt volcanoes. Periodic surveys are more appropriate for volcanoes with longer repose times, for remote volcanoes where instrument installation and maintenance can be challenging, and for measuring the whole chemical-isotopic spectrum of volcanic fluids. Over the years, geochemical monitoring has progressively transitioned toward the implementation of permanent instrumental networks, and this evolution is well represented in the two previous editions of the Encyclopedia of Volcanoes. In the first edition (2000), Delmelle and Stix [9] discussed the processes governing the temporal variability of volcanic gas composition mostly relying on the results of periodic direct sampling of fumaroles. In the same volume, Stix and Gaonach [10] elaborated on initial instrumental attempts to remotely measure plume composition

(by Fourier Transform Infrared Spectroscopy, FTIR), and the volcanic SO_2 flux from either ground (using the Correlation Spectrometer, COSPEC) and space (using the Total Ozone Mapping Spectrometer, TOMS). In the second edition, Fischer and Chiodini [5] still heavily elaborated upon the results of direct fumarole sampling, discussing isotopic evidence for the origin of elements (C-H-O-S-N-halogens-noble gases) in volcanic gases, and presenting a comprehensive discussion on thermodynamic techniques used to estimate hydrothermal P-T conditions from hydrothermal gas equilibria in the H_2O-H_2-CO_2-CO-CH_4 system (the reader is referred to this study for a detailed discussion of both topics). However, they also increasingly discussed the application of instrumental techniques in geochemical volcano monitoring.

The core focus of the present chapter is to review the most recent technological and science advances in volcanic gas monitoring.

2. **Drivers of change: what controls geochemical changes.**

Interpreting the time series streamed by a geochemical volcano monitoring network requires that a coherent understanding is available for the processes that drive change in fluid chemistry/flux (Fig. 1). This knowledge also serves as a guide for the establishment of the monitoring network, and for selecting the ideal parameters to monitor. Key to success is a robust knowledge of baseline composition/flux levels (to be acquired during volcano repose or background eruptive activity) – this is needed to identify change. We review below the key drivers of change at play at volcanoes.

2.1 Strong Volcanic Gas Emitters: change due to magmatic degassing processes.

With the term Strong Volcanic Gas Emitters (SVGE), we refer to those volcanoes whose gas emissions have regularly (or frequently) been detected from space in the last decades of satellite observations. This category includes a broad spectrum of volcanoes, such as (i) open-vent, persistently degassing mafic volcanoes and (ii) more silicic volcanoes that are (or have recently been) in eruption or are soon to erupt, and therefore host high-temperature (>> 600 °C) crater fumarole fields (Fig. 1a). At these volcanoes, the critical process that imparts compositional variability in volcanic fluids is the selective/sequential vapor partitioning of the various volatiles during magma degassing (Fig. 1a). Magma degassing, the process through which volatiles exsolve from silicate melt and separate into a vapor phase (bubbles), is a universal process associated with magma ascent and decompression (decompressional degassing) and/or crystallization (second boiling) [4,6]. At any P-T-X condition, the magmatic volatile species have distinct solubilities and vapor/melt partitioning behaviors. The less soluble volatiles (Ar, N_2>CO_2 >He) partition into the volatile phase earlier (deeper) than more soluble ones ($H_2O \approx S <$ halogens) [6], so the chemical ratios between the species evolve during magma decompression (ascent) [11]. Geochemists exploit this degassing pattern to monitor changes in magma degassing depth/conditions from changes in gas ratios (e.g., Ar/CO_2, CO_2/He, CO_2/S, CO_2/H_2O, S/Cl) in monitored surface fluids. This directly applies when surface fluids are purely magmatic in nature, i.e.,

129 directly derived from magma without any re-equilibration or hydrothermal alteration
130 (see below). Solubility-dependent degassing patterns are thus mainly explored in
131 magmatic emissions from SVGE (Fig. 1a), or in WVGE that are transitioning into
132 eruption (where degassing signals may be more confused as masked by
133 hydrothermal interactions, see below). Magmatic gases are essentially mixtures of
134 major species H_2O, CO_2, and SO_2 (H_2S normally makes a small fraction of total
135 sulfur S_t: Fig. 1b), plus a plethora of minor and trace species. While inter-volcano
136 variations in H_2O-CO_2-SO_2 proportions mostly reflect different geodynamic setting
137 (that is, melt compositions and volatile contents; [4]), temporal changes at
138 individual volcanoes have been shown to be caused by and indicative of changing
139 magma degassing conditions. In particular, increasing CO_2/SO_2 ratios have now
140 been observed prior to eruption at many mafic and silicic volcanoes worldwide.
141 This reflects the precursory surface release of deeply exsolved CO_2-rich gas,
142 separately ascending from soon-to-erupt mafic magma at depth [8, 11] (Fig. 1a,
143 b).

144 In addition to chemical composition, gas fluxes (e.g., the mass of gas emitted per
145 unit time) also change in response to pre-eruptive magma accumulation/ascent
146 and degassing. This is easily understood in the specific case of the SO_2 flux (ΦSO_2,
147 in kg/s), the most easily measurable volatile (see 3.3), from the relationship:

148 $$\emptyset_{SO2} = Q_{in} \cdot 2\Delta X_S \cdot (1 - x) \cdot \rho_m$$

149 where Q_{in} is the magma input rate (in m^3/s) above the level (depth/pressure) at
150 which effective sulfur degassing starts (typically 4-9 km below the volcano top for
151 mafic magma [6]), ΔX_S is the bulk mass loss of elemental sulfur upon degassing
152 (e.g., the difference between parental melt and residual S content in degassed
153 magma), and *x* and ρ_m are melt crystallinity and density (in kg/m^3) (the coefficient
154 2 = 64/32 is required to covert S mass into SO_2 mass). When magma supply (Q_{in})
155 to the volcano feeding system increases in the eruption run-up, the SO_2 flux
156 escalates in advance to magma eruption, either because gas bubbles are buoyant
157 enough to separately ascend through the melt or because they can escape via a
158 permeable gas bubble network. Note that the same equation is used to convert
159 measured SO_2 fluxes into Q_{in} using petrological estimates of S contents in melt
160 inclusions and matrix glasses [4].

161 2.2 Weak Volcanic Gas Emitters: change due to magmatic-hydrothermal
162 reactions.

163 Closed-vent, dormant/quiescent stratovolcanoes and calderas (Fig. 1c) are
164 normally classified as Weak Volcanic Gas Emitters (WVGE) as they typically lack
165 large atmospheric plumes that can be detected from space. Their most visible
166 degassing manifestations are relatively cold (typically close-to-boiling
167 temperature) fumaroles and steaming grounds/soils [1]. During volcano repose,
168 these manifestations typically exhibit stable hydrothermal signatures, being
169 dominated by steam (generally > 90 mol. %) plus 1-10 mol% gas essentially
170 consisting of a CO_2+H_2S mixture [5, 9], plus minor N_2, Ar, H_2, CH_4, and CO, but no
171 (or minimal) SO_2 and HCl (exceptions of SO_2 and HCl-rich hydrothermal gases

exist, however). These S-poor (Fig. 1b) hydrothermal vapors are generally formed by boiling of (meteoric water- or seawater-fed) aquifers heated by a magma source at depth, but they usually contain a magmatic volatile component as well, as evidenced by isotopic evidence (primarily $^{13}C/^{12}C$ and $^{3}He/^{4}He$ ratios; [6]). Hence, at WVGE volcanoes, chemical changes are mainly driven by the extent and dynamics of hydrothermal-magmatic fluid interactions [11]. If the volcano becomes restless, geochemists carefully examine fumarole compositional time series to identify any increase in the magmatic gas proportion, as indicated for example by increasingly CO_2-S-rich and less water-rich compositions (Fig. 1b). Complications arise, however, as the magmatic S supply can be masked by scrubbing (the sequestration of SO_2 and H_2S - and other reactive gas species - into hydrothermal solutions/minerals, owing to their high water solubility and reactivity to host rocks), and because sulfur may instead be contributed by destabilization of S-bearing hydrothermal minerals in the volcano heating phase (Fig. 1c). This makes inert gases (N_2, noble gases) and their isotopic ratios more sensitive tracers of an increasingly magmatic signature of fluids [5]. Compositional change is also determined by evolving hydrothermal P-T conditions, driven by increasing supply of hot magmatic gases. This evolution can be monitored by modeling H_2O-H_2-CO_2-CO-CH_4 equilibria (Fig. 1d) that are extremely sensitive to P-T-redox conditions [5]. While remote SO_2 flux measurements are ineffective during quiescence and early unrest phases at WVGE, due to nil or weak SO_2 release, soil gas monitoring and airborne plume CO_2 surveys can allow early detection of increasing supply of magma-sourced CO_2.

3. Sentinels of change: techniques in geochemical monitoring

An appropriate volcano monitoring strategy requires the combination of different techniques into an integrated observational network (Fig. 2). It is important to keep in mind that the fluid manifestations vary with volcanic activity status and style [1], implying that the choice of methods/instrumentations to prioritize may vary as a volcano becomes increasingly restless (Fig. 2). This section describes the principal geochemical techniques used and their respective contributions to volcano monitoring (with some selected case studies).

3.1. Fumarole direct sampling.

Although gas monitoring is increasingly realized using real-time instrumental networks (Fig. 2), direct sampling remains an invaluable source of information, as it is the only tool that allows for a full characterization of the volcanic gas composition, including minor and trace elements and isotopes. Direct sampling involves collection of fumarole gases using Giggenbach's alkaline solution method [3, 5]. In this process, fumarolic gas stream is channeled (via a quartz tube) into a pre-evacuated and pre-weighed flask filled with 4 M NaOH. Fumarolic gases bubble through the alkaline solution, causing water vapor to condense, and CO_2 and acidic gases (HCl, HF and S species) to dissolve in the solution. Non-condensable gases (H_2, N_2, CO, and CH_4) and noble gases are hence concentrated in the flask headspace.

Water, the most abundant magmatic volatiles, is difficult to measure in plumes (cf. 3.2), because of the high and variable atmospheric background. Hence, direct sampling is the key tool to reliably detect the gas/steam (CO_2/H_2O) ratio increase [12] that typically tracks the increasing magmatic (over hydrothermal) fluid contribution as a volcano becomes restless (see also the Turrialba example [13] illustrated in Figure 1b). Direct sampling can also capture hydrogen and oxygen isotope compositions normally becoming increasingly heavy (δD and $\delta^{18}O$ becoming more positive) as fumarolic steam transitions to having a greater proportion of magmatic relative to meteoric water [14]. Resolving the magmatic vs. non-magmatic fluid (meteoric, atmospheric, biogenic) contributions becomes especially effective when a multi-isotope approach is employed, in which tracers such as C ($\delta^{13}C$; Fig. 3), N ($\delta^{15}N$), He ($^3He/^4He$), and Ar ($^{40}Ar/^{36}Ar$) isotopes (to cite only the most frequently used) are measured in concert [6]. The isotopic compositions of such elements allow quantification of the magmatic gas influx, to infer volatile origin, and to characterize the physico-chemical processes of magma degassing, gas migration, and interaction with groundwaters. Noble gases ($^3He/^4He$, $^4He/^{20}Ne$, and $^{40}Ar/^{36}Ar$ ratios) are especially useful in this exercise, because of their inert nature, and because of the contrasting signatures of magmatic, crustal and atmospheric sources.

In addition to isotopes, a series of chemical tracers are effectively monitored by direct sampling to track unrest, and potentially forecast activity resumption at closed-vent volcanoes. For example, as magma migrates toward the surface, scrubbing of magmatic S and Cl by hydrothermal reactions [15] will be reduced or minimized, which can be detected by decreasing CO_2/S ratios (Fig. 1, 4), change in S speciation (increases of magmatic SO_2 over hydrothermal H_2S) and increasing halogens ($HCl+HF/CO_2$) (Figs. 3 and 4). Also, the minor carbon species, and the proportion relative to CO_2 are especially useful as they are sensitive to temporal changes in pressure and temperature conditions of the hydrothermal system. As a rule of thumb, the CO/CO_2 and CO_2/CH_4 ratios both increase (Fig. 1d) as the magmatic gas influx increases, and hence the hydrothermal system is driven to higher temperature and eventually more oxidized (magmatic) conditions.

Case study box: Peteroa and Pico de Fogo

Over the past decade, extensive crater fumarole time series have been obtained by direct sampling that have not only identified precursors to eruption, but also revealed the intricate processes that control volcano dynamics. Direct sampling has made significant strides in understanding the compositional variations before and during eruptions. Two notable cases in which gas parameters have contributed to effectively identify processes and likelihood of eruption are those of Peteroa volcano (Argentina-Chile) and Pico do Fogo (Cape Verde) (Figure 3).

Peteroa is a typical andesitic WVGE stratovolcano with fumaroles at near boiling temperatures. During 2010 to present, the volcano has experienced two mildly explosive (Volcanic Explosivity Index, VEI =2) eruptions in 2011 and 2018-2019 (Fig. 3a). Regular fumarole direct sampling contributed to tracking the quiescence-to-eruption transition by distinguishing clear switches from hydrothermal to

magmatic compositions. During quiescence, gas composition was typically in the hydrothermal domain, as indicated by low HCl/CO_2 and SO_2/H_2S ratios (Fig. 3a). In contrast, in the pre-, syn-, and post-eruptive phases, SO_2, HCl, and HF increased significantly, causing the SO_2/H_2S, HF/CO_2, and HCl/CO_2 to simultaneously increase by orders of magnitudes (Fig. 3a), and implying minimal (or reduced) magmatic gas scrubbing and more oxidizing redox conditions (as typical of magmatic conditions). This redox evolution before the phreatomagmatic eruption was also detected using the CH_4/Ar ratio. During quiescence, the CH_4/Ar ratio was high, indicating reducing conditions and low temperatures (Ar was largely meteoric Ar, as indicated by $^{40}Ar/^{36}Ar$ ratios slightly above the 295 air ratio). The CH_4/Ar ratio then decreased in the 2018-2019 magmatic phase (Fig. 3a), indicating CH_4 was depleted at a faster rate (prevalence of oxidizing, magmatic conditions) relative to Ar.

Similar changes in gas composition were observed before the 2014-2015 eruption of Pico do Fogo volcano [17] (Figure 3b), a mafic alkaline volcano in the Cape Verde archipelago hosting a summit hydrothermal system feeding a swarm of crater fumaroles with temperatures up to 350°C. The fumarolic CO/CO_2 and H_2/CO_2 ratios started to increase in 2009-2010 (marking the onset of a “magmatic reactivation” phase). These variations were interpreted [17] as caused by an escalating input of deeply sourced, CO_2-rich magmatic gases that ultimately caused heating of the hydrothermal system. This heating phase manifested in a remarkable increase of estimated equilibrium temperatures (Eq.T in Figure 3b), from circa 200 to circa 500°C (as inferred from CH_4-CO-CO_2 geothermal gas geothermometer [5]). The isotopic composition of $\delta^{13}C–CO_2$ (in ‰ vs. VPDB, Fig. 3b) peaked at the eruption onset, implying involvement of an isotopically heavier (more magmatic) CO_2 source, associated with the volatile-rich erupting magma.

3.2. In-situ plume measurements

At open-vent volcanoes, direct fumarole sampling becomes increasingly ineffective since the gas output is dominantly sustained by large atmospheric plumes [1]. Monitoring hence requires plume measurements. In-situ measurements are made after the gas has exited the crater and been diluted by atmosphere. The two most common in-situ plume techniques are chemical traps and Multi-GAS measurements. Both techniques rely on a pump to draw volcanic gases into the instrument.

Chemical traps use compounds that react with acid volcanic gas species to take samples of volcanic plumes. The most used technique is the filter pack method, whereby plume gas is pumped through a series of filters impregnated with alkaline solutions such as K_2CO_3 or NaOH with glycerol to enhance the absorption efficiency. This method is convenient for rapid sampling of plumes, but care must be taken not to saturate the filters or gas concentrations and ratios will not be representative. Saturation can be avoided using bubblers, which involves pumping plume gas through glass flasks with a fritted tip submerged in an absorbing solution. The Rashig tube (involving pumping gas through a rotating glass tube filled with glass rings and an absorbing solution) and denuders (glass tubes coated

with an interior coating of reactive compounds, through which gas is pumped to sample reactive halogen species) have also recently been used.

The most-commonly used method for real-time in-plume measurements is the Multi-GAS. In Multi-GAS instruments, the air-diluted volcanic gas is passed through a series of electrochemical and/or non-dispersive infrared (NDIR) sensors. Each sensor measures the concentration of a target gas species in the mixture. The number and specificity of sensors used varies greatly between Multi-GAS designs. CO_2 is typically measured by an NDIR sensor, H_2O by an NDIR or derived from a relative humidity sensor, while SO_2, H_2S, CO and H_2 are typically measured by specific electrochemical sensors (H_2 can also be measured by a semi-conductor sensor). Br and Cl electrochemical sensors have also been tested with mixed results so far. All sensors must be calibrated for response (and cross sensitivity) prior to use in the field, and frequent re-calibration of the permanent instrument is required to correct for any drift. Each sensor has a specific calibration range and care must be taken not to oversaturate it. Since its first deployment, the Multi-GAS has quickly become the most widely used instrument for measuring the chemical composition of volcanic plumes, both during campaign measurements and in permanent deployments. The main advantages of the system are its robustness, low cost, near real-time results, and its ability to acquire data autonomously at a frequency of 1Hz. The Multi-GAS technique is particularly well suited for permanent installations. Dozens of active volcanoes currently have permanent Multi-GAS units monitoring the composition of their volcanic gases in real time.

Both the filter pack and the Multi-GAS instrument provide ppmv concentrations of gas species, which are then converted into molar ratios. The ratio of all species to a common denominator allows the complete gas composition to be determined. Volcanic gas composition is a complex function of (1) parent melt composition and volatile content, (2) exsolution and gas separation depth/pressure, (3) temperature, (4) oxidation state, and (5) hydrothermal interactions. Changes in volcanic gas composition over time have therefore been related to changes in any one or a combination of these parameters and have now been observed at multiple volcanoes both during and prior to eruption.

Case study box: Turrialba

A remarkable example of how fumarole (direct sampling) and plume (Multi-GAS) monitoring can integrate to capture activity escalation in the run-up to eruption has recently been offered by Turrialba (Costa Rica). Geochemical monitoring of Turrialba over the last quarter century has documented a spectacular transition from hydrothermal to magmatic gas compositions preceding phreatomagmatic to magmatic eruptions (Figure 4). This monitoring period also spanned the technological advent of the Multi-GAS. Prior the mid 1990s Turrialba had been dormant for almost one and half centuries, and the reactivation of the magmatic system occurred slowly, allowing an unprecedented characterization of the changes in gas emissions that are expected at any volcano where a hydrothermal system is displaced by magma emplacement preceding an eruptive period.

Direct sampling of the West crater fumaroles between 1998 and 2008 [13] showed gradual and unequivocal changes in gas compositions from hydrothermal to magmatic signatures. Hydrothermal gases were characterized by CO_2/S_t (where S total = $H_2S + SO_2$) > 100, H_2S/S_t = 1 and very low halogen contents. CO_2/S_t reached a peak in late 2001 early 2002, the first indication of deep magma injection, marking the beginning of radical changes toward magmatic gas compositions. By 2007-2008, the CO_2/S_t ratio had dropped by 3 orders of magnitude, H_2S/S_t had decreased to essentially zero, and $(HCl+HF)/CO_2$ had increased by >2 orders of magnitude. By this time, small vent-opening eruptions occurred in 2010, 2012 & 2013, making direct sampling of the fumaroles in the west crater too dangerous.

A Multi-GAS station was installed at the summit in early 2014, just in time to record changes in the plume gases prior to the violent phreatic eruption of October 2014 and the subsequent progression into phreatomagmatic eruptive activity in 2015 [18]. Clear peaks in CO_2/S_t were observed in the weeks preceding the first three eruptive phases (black stars Figure 4), indicating that deep magma injection was driving the activity. The baseline H_2S/S_t ratio prior to and between the initial eruptive episodes was ~0.5, higher than that observed in the highest temperature fumaroles of the West crater in 2008, and consistent with the idea that the Multi-GAS was measuring bulk gas emissions from diverse fumarolic/vent sources within the crater. From mid-2014 to late 2015 the H_2S/S_t and CO_2/SO_2 ratios varied wildly, indicating instability of the system and expulsion of the hydrothermal system by intruding magma (period A, Figure 4).

The process of vent opening and displacement of the hydrothermal was completed by early 2016, and gas compositions changed abruptly to purely shallow magmatic in character, with $CO_2/S_t < 5$ and $H_2S/S_t < 0.1$ (period B, Figure 4). The summit Multi-GAS site was no longer sustainable, and a station was installed on the lower flank. Eruptive activity gradually transitioned from violent explosions to dominantly open-vent ash emissions, and in late 2016 and early 2017 small magmatic Strombolian eruptions started occurring, continuing until late 2018. As activity waned in 2019-2020, H_2S/S_t and CO_2/S_t rose significantly, indicating the initiation of the re-establishment of the hydrothermal system (period C, Figure 4).

3.3. Ground-based remote plume measurements

Remote sensing, wherein absorption of radiation at specific wavelengths by volcanic gases of interest is leveraged in lieu of directly measuring or sampling gas, is a crucial modern subdiscipline of volcanic gas monitoring. In addition to providing data not obtainable by direct measurements (e.g., gas flux), remote sensing measurements also offer safer opportunities for volcanologists to measure magmatic gas compositions and fluxes in real time even during violent eruptive activities.

Many of the major volcanic gas species have absorption features in the ultraviolet (UV) and/or infrared (IR) parts of the electromagnetic spectrum that are sufficiently distinct to be resolved by remote sensing [1,6,7]. SO_2 has strong absorption

features in both the UV and IR, and its negligible (ppb) levels in the background atmosphere make it the easiest volcanic gas to measure by ground-based remote sensing. H_2O, CO_2, CO, HCl, HF, SiF_4, and OCS all have absorption features in the IR and have been measured using open-path Fourier transform infrared (OP-FTIR) spectrometers. Isolation of volcanic H_2O and CO_2 signals from the atmospheric background can be problematic but can be achieved by using their concentration ratio to purely volcanic species (SO_2, HCl). Typically, a hot IR source (the magma itself in most applications) and low ambient air H_2O contents are required. Some attempts have also been made to measure H_2O in the visible and UV ranges. H_2S, despite a shortwave UV absorption feature, is typically difficult to measure unless an active source, such as a UV lamp, is used. H_2 has not been measured by either UV or IR remote sensing so far. HBr itself has also not been measured, but once oxidized to BrO can be measured in the UV.

The volcanic SO_2 flux is one of the principal monitoring datasets at many active volcanoes. The amount of SO_2 emitted is inextricably linked to the type of volcano and how it behaves [1], and, in many cases, SO_2 fluxes can be used as a rough proxy for eruptive activity levels.

Ground-based SO_2 flux measurements most often utilize UV differential optical absorption spectroscopy (DOAS), either via a single spectrometer, a network of multiple spectrometers, or integrated into a SO_2 camera. In either cases, the amount of gas between the spectrometer and the radiation source is derived via the Beer-Lambert law. Single-spectrometer measurements are inherently limited in temporal resolution, given the finite time necessary to complete a scan or traverse (every few minutes at best), which can limit integration with data of higher temporal resolution (e.g., seismicity or infrasound). The resolution of SO_2 flux datasets can be improved, however, by utilizing spectrometers in other configurations. Networks of scanning or static upward-looking spectrometers offer SO_2 flux measurements at up to ~1 Hz. Similarly, spectrometer-integrated SO_2 camera also offers high-resolution of SO_2 fluxes, but with the added benefit of a synoptic view of plume behavior, which provides important context for interpreting degassing dynamics. High spatial resolution allows resolving emissions from individual vents.

OP-FTIR spectroscopy provides information on additional gas species using natural IR sources, such as lava or the sun, or active sources, such as IR lamps. If the path-length is known, average gas concentrations may be calculated; often, results are instead presented as molar ratios of gas species. Measurements made via OP-FTIR have been utilized at high temporal resolution (up to 1 Hz) to investigate rapid, short-term changes in gas chemistry correlated with rapid changes in eruptive dynamisms [18], as well as with geophysical signals. They can also be used to monitor plume degassing at open-vent volcanoes over longer periods. Ratios of different gas species to SO_2 can be leveraged alongside independently measured SO_2 fluxes to quantify the of each gas species and bulk gas fluxes. The wide range of gases that can be measured via OP-FTIR includes a number of redox couples (e.g., CO_2/CO) that can also provide information on changing redox conditions and degassing style.

Case study box: Cotopaxi and Kīlauea.

Often, as dormant or quiescent volcanoes begin to build toward renewed activity, one of the quantifiable manifestations of the reawakening is an increase in SO_2 emissions. This has been documented for many eruptions, including Pinatubo (Philippines, 1991), Mount St. Helens (USA, 2004), Redoubt Volcano (USA, 2009), and others. More recently, the 2015 eruption of Cotopaxi (Ecuador) – the first since the 1940s – exhibited a precursory increase in SO_2 emission as detected by their network of scanning DOAS spectrometers [19]. Since 2008, the two permanent DOAS scanners have measured SO_2 fluxes with a temporal resolution of ~10 minutes. Beginning in mid-May of 2015, ~6 weeks after an initial increase in seismicity, SO_2 emissions began to climb from ~30 to ~300 t/d. From the end of May through the onset of explosive eruptions in mid-August, SO_2 emissions increased further and varied between a few hundred and a few thousand t/d. BrO was detected beginning in June as discrete seismic events began to transition to tremor, and HCl was detectable by FTIR by early August. During the months-long eruptive period from August through November, SO_2 emissions were still higher, averaging ~3,000 t/d, with individual measurements up to ~25,000 t/d. The precursory sequence of combined seismic and gas data was interpreted to be the manifestation first of shallowing magma that was still deep enough to inhibit most sulfur exsolution, followed by further shallowing of the magma, which brought about the onset of enhanced sulfur degassing and measurable halogen degassing.

While the Cotopaxi eruption is an example of increasing SO_2 emissions during precursory unrest after decades of quiescence, a number of volcanoes also show the opposite. A decrease in SO_2 emissions ahead of explosive activity, a sign of sealing and pressurization, on timescales of minutes to days or weeks – as measured by SO_2 camera or DOAS network – has been documented at systems including Fuego (Guatemala), Galeras (Colombia), Popocatépetl (Mexico), Karymsky (Russia), and Sinabung (Indonesia).

Though less common at basaltic, non-arc systems – because of the high solubility of sulfur in basalt [4] that typically limits sulfur degassing to very near-surface ($\lesssim$500 m) – changes in SO_2 emissions can also sometimes herald changes in eruptive activity at such volcanoes. In late 2007 through early 2008, even as a decades-long rift eruption of Kīlauea (USA) continued, summit SO_2 emissions – measured routinely since the 1970s – began to increase over the course of a few months, from ~200 to ~1500 t/d [20]. There was a concurrent decrease in the CO_2/SO_2 ratio of the summit gases; seismic activity in the summit area increased as well, preceding the onset of the SO_2 increase by ~1 month. Thus, gas and seismicity appeared to hint at potential eruptive activity. There was, however, no shallow (1-2 km) inflation, which would normally be expected in advance of an eruption. To the contrary, a deflationary trend that began more than a year prior continued unchanged. An incandescent fumarole field developed after ~3 months of increasing SO_2 emissions; the vent-clearing explosion, which formed a new crater and marked the onset of a decade-long summit lava lake eruption, took place a week later. In this case, where deformation seemed to indicate otherwise,

the progressively increasing SO_2 emissions indeed were a key precursor to the new eruption for Kīlauea.

3.4. Satellite-based remote plume measurements.

Satellite measurements complement ground-based volcanic gas monitoring by covering larger spatial scales (regional to global), ensuring geochemical surveillance of otherwise unmonitored volcanoes, and providing observations when conditions become too hazardous for proximal data collection (e.g., during the precursory phase of major eruptions) [21]. Satellite and ground-based remote sensing of volcanic plumes rely on the same fundamental principles, i.e., observing the absorption of electromagnetic radiation in the UV and IR spectral bands by volcanic gases and using this to quantify atmospheric column amounts of the target gas species. Routine, satellite-based geochemical monitoring of volcanic gases in lower tropospheric plumes (i.e., passive degassing) is currently restricted to SO_2 and possibly BrO [6,21]; a more extensive suite of gas species can potentially be detected in eruptive emissions (e.g., CO_2, CO, HCl, OClO) due to a combination of higher plume altitude, larger gas amounts, and more accessible absorption bands. UV satellite instruments have greater sensitivity to lower tropospheric SO_2 than IR sensors, and so the former are favored for space-based monitoring of volcanic emissions but are limited by the availability of UV radiation. IR sensors provide critical observations during the night and at high latitudes in the winter months.

Satellite measurements of volcanic plumes offer several advantages over other monitoring techniques. They provide daily, near-global coverage of volcanic degassing and some satellite missions, in operation since the early 2000s, now provide unique, multi-decadal time series of SO_2 emissions from SVGE volcanoes. Two decades of UV measurements by the Ozone Monitoring Instrument (OMI) on NASA's Aura satellite have permitted the compilation of a comprehensive inventory of ~100 SVGE volcanoes characterized by persistent SO_2 emissions (Figure 6), providing new constraints on the global volcanic SO_2 flux and on the fluxes of other volcanic gases (e.g., CO_2) when combined with in-situ measurements of gas ratios. The OMI SO_2 inventory (Figure 6), now being integrated with results from the more recent TROPOMI, provides a snapshot of global volcanic degassing, including persistent, high SO_2 fluxes from many open-vent SVGEs (e.g., Etna, Manam, Popocatepetl), some abrupt changes in SO_2 emissions at SVGEs that host basaltic lava lakes (e.g., Ambrym, Kīlauea, Nyiragongo), and notable recent trends toward higher SO_2 emissions at some volcanoes (e.g., Sangay, Sabancaya). In addition to detecting any significant changes in SO_2 flux at SVGEs, satellites also permit rapid identification of any new SO_2 emissions (above detection limits, which may be on the order of 100s of t/d SO_2 or more) from previously inactive volcanoes, such as WVGE volcanoes in transition to a more active state. Such data can be used to assess the need for increased geochemical surveillance via deployment of ground-based instrumentation. Unlike many ground-based UV spectrometer networks at degassing volcanoes, satellite-based detection of volcanic SO_2 plumes is insensitive to wind direction. Furthermore, all satellite data from a given sensor are

processed using the same SO_2 retrieval algorithm, providing a level of consistency (and the opportunity for reprocessing as algorithms improve) lacking in ground-based remote sensing data collected using a variety of instruments.

Disadvantages of satellite observations include lower sensitivity to volcanic SO_2 than ground-based measurements, a reliance on relatively clear observing conditions (meteorological clouds often partly or completely obscure volcanic plumes at lower altitudes), and relatively low temporal resolution. The satellite orbit governs the temporal resolution of the measurements, and most UV and IR sensors measuring volcanic SO_2 operate in polar orbit, typically providing data only once or twice per day at low latitudes. However, over the coming decade a new constellation of geostationary UV satellite sensors will provide hourly SO_2 measurements in daytime for some volcanic regions (North America, Europe and East Asia). Satellite measurements of SO_2 are also typically reported as SO_2 mass rather than SO_2 flux, in contrast to ground-based SO_2 data, hence merging the two datasets can be challenging. Various techniques are being refined for estimating SO_2 fluxes from satellite observations.

Case study box: Fourpeaked Mountain and Merapi

Timely detection of new SO_2 emissions at reawakening, unmonitored volcanoes is critical, as it can be diagnostic of magmatic intrusions that may progress toward eruption, prompting a major reassessment of potential volcanic hazards. Long-dormant volcanoes (e.g., WVGEs) typically host extensive hydrothermal systems that may initially scrub SO_2 before the hydrothermal fluids dry out and SO_2 emissions increase. In September 2006, ice-clad Fourpeaked Mountain (USA), thought to have been inactive in the Holocene, produced an ostensibly phreatic eruption that nevertheless emitted SO_2 (~2000 tons) clearly detected from space by Aura/OMI. This satellite data and other observations prompted increased surveillance of Fourpeaked Mountain by the U.S. Geological Survey Alaska Volcano Observatory (USGS/AVO), including the installation of a seismic network and further airborne volcanic gas measurements. Fourpeaked Mountain now ranks as an historically active volcano, despite not appearing on the list prior to 2006. Similar, potentially 'vanguard' SO_2 emissions were detected by Aura/OMI at Garbuna volcano (Papua New Guinea) in October 2005; the first known historical eruption from a volcano whose last major eruption was about 1800 years ago.

The significance of these small but measurable SO_2 emissions is not yet fully understood, although activity at Fourpeaked Mountain has been ascribed to a shallow magmatic intrusion that stalled, cooled, and degassed in the upper 10 km of the crust. It has been suggested that the discharge of >100 t/d SO_2 should be regarded as diagnostic of magma intrusion, rather than the expulsion of gas from pressurized hydrothermal systems, since SO_2 is not easily extracted from hydrothermal fluids. Small SO_2 emission events without significant discharge of juvenile magma could be regarded as 'failed eruptions' and may be common in the life cycle of a volcano, but it is only very recently (the last two decades) that satellite observations capable of detecting such events have become available.

Satellite measurements also enable detection of significant changes in SO_2 emissions at active volcanoes. Prior to major explosive eruptions, conditions can become challenging for ground-based remote sensing (e.g., due to destroyed equipment; extensive, ash-laden plumes; or evacuations preventing access to instruments and/or roads), or increasingly vigorous emissions may drift beyond the range of ground-based spectrometer networks. During precursory unrest before the major November 2010 eruption of Merapi volcano (Indonesia), satellites played a key role in monitoring increased SO_2 emissions [22]. In late October 2010, seismicity at Merapi increased and a time series of SO_2 emissions derived from satellite measurements showed fluxes greatly exceeding both background and eruptive emissions recorded at Merapi between 1986 and 2007, indicating the ascent of fresh, mafic magma in advance of the paroxysmal phase of the eruption on November 4, 2010. SO_2 emissions temporarily declined to a relatively low level (but still at elevated levels relative to previous Merapi eruptions) during the growth of a lava dome on November 1-3, 2010, but ramped up again significantly on November 3, and peaked during the climactic explosive eruptions of November 4-5.

3.5. Soil degassing

At closed-vent volcanoes, the largest fraction of the magmatic volatile output is not sustained by crater fumaroles/plumes, but rather by more “invisible” diffuse emissions from degassing soils. Soil degassing from volcano summits, flanks and peripheries hence represents a sensible tool to monitor changes in volcanic activity. CO_2 is the main soil gas constituent, and monitoring the soil CO_2 flux contributes to understanding volcano behavior and state.

The soil CO_2 flux is the result of two different processes [23]: diffusion and advection. Molecular diffusion is the process in which gas is transported from a region of high concentration to a region of low concentration. Advection is the process where gas is transported in response to a pressure gradient. Gas transport occurs by a combination of these two processes and the total flux is the sum of the advective and diffusive components. Generally, low CO_2 fluxes are associated with diffusion, whereas high values occur when advection is the prevalent gas transport mechanism. Soil degassing is typically structurally controlled, with fractures and faults acting as main pathways of gas transport and surface release. Mapping of soil CO_2 emissions at volcano-scale is hence a convenient method for identifying structural lineaments and faults related to the regional or local tectonic setting.

The soil CO_2 flux is typically measured by the accumulation chamber method, which uses the temporal dependence of CO_2 concentration inside a closed chamber placed above the ground to calculate a flux [23]. The accumulation chamber can be applied either (i) during periodic soil surveys, in which measurements are carried along a regular grid to identify anomalously degassing Diffuse Degassing Structures (DDS) and hence measure their total CO_2 flux (in units of tons/d) or (2) by fully automated, permeant instrument measuring in near real-time the site-specific CO_2 flux (expressed in g m^{-2} d^{-1}), and its changes through

time. While (i) is especially useful for mapping, and for reconstructing volatile output budgets, methodology (ii) is especially useful for volcano monitoring.

Case study box: Stromboli and El Hierro

Continuous accumulation chamber measurements have proven especially useful for capturing escalating soil CO_2 fluxes in the run-up to eruption. At Stromboli, an open-vent volcano in the Aeolian archipelago (Italy), persistent mild (Strombolian) explosive activity is occasionally interrupted by potentially tsunamigenic explosive (paroxysmal) and effusive eruptions, the most recent of which occurred in 2002-2003, 2007, 2014, and 2019. Continuous soil CO_2 fluxes, acquired since 1999 with automatic accumulation chambers on the volcano's summit, have been especially useful to characterize, and eventually forecast, the Strombolian-to-effusive activity transition [24] (Fig. 7a). The volcano's CO_2 output is modulated by a delicate dynamic balance between the rate of magma supply and degassing in the plumbing system, and the rate of CO_2 surface release from the plume, soils, and thermal aquifer (Fig. 7b). Increasing CO_2 flux is a hint for escalating CO_2 supply from ascending, volatile-rich magma. Elevated CO_2 fluxes (up to 30,000 g m^{-2} d^{-1}) were repeatedly observed prior to effusive eruptions in 2002-2003, 2007, and 2014 (Fig. 7b). Also, CO_2 fluxes progressively increased from 2005 to 2019, at an average rate of 4.1 g m^{-2} d^{-1}, and even more substantially (at a rate of 24.2 g $m^{-2}d^{-1}$) since 2016. Very high fluxes, up to 24,000 $gm^{-2}d^{-1}$, were again detected in the months prior paroxysmal activity in July 2019.

CO_2 flux surveys in anomalous areas (and total CO_2 flux quantifications) can also be useful for monitoring purposes. For example, more than 17,000 diffuse CO_2 flux measurements were carried out [25] before and during the 2011-2012 volcanic eruption of El Hierro, the smallest and south-westernmost island of the Canarian archipelago. Two significant CO_2 flux increases were recorded, during the pre-eruptive and eruptive phases, respectively. The first CO_2 flux increase was recorded two weeks before the onset of the submarine eruption (time set at 0 in Figure 7c) with an estimated average CO_2 output (627 t d^{-1}) well above the background (422 t d^{-1}). This increase was likely due to the precursory release of CO_2-rich magmatic gases, sourced by deeply rising magma. The second increase started coincident with the most energetic syn-eruptive seismic activity (see Figure 7c) interpreted to reflect relaxation around the magma reservoir that fed the eruption.

3.6 Volcanic lakes

Many closed-vent volcanoes are topped by colorful crater lakes that, when present, are a primary target of geochemical monitoring. Volcanic lakes [26] are surface manifestations of complex processes occurring in the hydrothermal-magmatic system. Lake chemistry results from a combination of volcanic gas injection, water-rock interaction, dilution by meteoric water, evaporation/degassing, mineral precipitation, drainage and recirculation of water from the lake into the underneath hydrothermal system. Hence, the physical (e.g., volume, temperature) and chemical characteristics (pH, compositions of dissolved, exsolved, and

precipitated constituents) of these lakes are variable because they reflect changes in both the sub-limnic hydrothermal system and the feeding magma source. Hyper-acid (pH< 1) hydrothermal fluids [27] can dissolve large quantities of fresh volcanic rock, creating porosity and permeability in the central up-flow zone, whereas secondary mineral precipitation seals fractures where fluid cooling and fluid-rock neutralization reactions take place. In acidic water (pH < 4), CO_2 can pass through crater lakes with minimal interaction (e.g., without being absorbed), whereas at high pH a large fraction of the magmatic CO_2 input can dissolve into water as HCO_3^-. Acidic magmatic gases, such as SO_2, HCl, and HF, are soluble in water and are absorbed in hydrothermal systems and/or volcanic lakes [15]; however, at hyperacidic lake conditions (pH < 1), associated with systems with high magmatic gas inputs, acidic gas species can also pass through the lake. Ultimately, gas fluxes from volcanic lakes depend on the balance between the magmatic gas input, and the capacity of the hydrothermal and limnic systems to absorb them. This balance is predominantly controlled by the volume of lake water relative to the magmatic gas influx, by the solubility of the gas species in question, and pH. Degassing through the surface of a volcanic lake occurs by bubbling (convective/advective degassing), evaporation and diffusion through the water/air interface.

Monitoring of lake level/volume, pH, temperature, dissolved components as well the lake gas emissions are effective ways of tracking changes in the hydrothermal-magmatic system. Injection of fresh magmatic fluids can trigger phreatic or phreatomagmatic eruptions, and is typically associated with increasing temperature, loss of lake volume, decrease in pH, increasing degassing of CO_2 and acid gases, and increasing concentrations of dissolved components in the lake, especially those derived from fresh intruding magma (such as Mg and rare earth elements). Hydrothermal sealing of the conduit, on the other hand, is driven by secondary mineral precipitation and decreased permeability, and can lead to gas accumulation and pressurization beneath the seal, potentially priming the system for larger eruptions once the seal fails catastrophically.

We summarize two distinct scenarios (Fig. 8) for the expected sequence of geochemical signals observable in the run-up to eruption at hyper-acidic crater lakes:

1. Eruption after a slow heating of the system due to magma injection. In this scenario, the crater lake system undergoes a gradual transformation. As magma infiltrates the subsurface, temperatures rise slowly, leading to subtle changes in the hydrothermal system. Over time, the lake's water temperature elevates until it evaporates. The injection of a fresh magma drives the Mg/Cl up (because of increased leaching of fresh magma) and increases the SO_2 flux (this increases further once the lake disappears). Initially, the lake plume CO_2/SO_2 ratio increases due to the deep magma recharge initiating the process and then decreases as the magma gets shallower. A further CO_2/SO_2 drop occurs at the time of the eruption as magma remobilizes S from the sublimnic alteration zone (Figure 8).

2. Sudden eruption triggered by failure of a hydrothermal seal. In this scenario, the crater lake system experiences a rapid and dynamic shift. Hydrothermal sealing causes pressure to accumulate and temperature to decrease. Temperature then increases once the eruption breaks the seal, and then the lake evaporates completely. Mg/Cl ratio remains constant until the seal breaks, which releases deeper Mg-rich fluids, and Mg/Cl further increases as the lake evaporates (and HCl is lost to the gas plume). SO_2 flux decreases as sealing occurs, then SO_2 flux increases moderately as the accumulated SO_2 is released. CO_2/SO_2 increases with sealing, then drops to shallow magmatic values as the seal breaks, and then goes back to background values (Figure 8).

The two scenarios above imply that a combination of regular surveys (for crater lake water sampling and analysis) and continuous observations with permanent instrumental networks (DOAS for SO_2 flux and Multi-GAS for plume chemistry) is critically required for effective lake monitoring.

4. A general, integrated model for volcano geochemical monitoring.

We synthesize the above information, and the results of monitoring efforts in response to recent volcanic unrests/eruptions, in the general model of Figure 9. The figure illustrates, in a simplistic, schematic and hence purely illustrative form, the expected sequence of geochemical changes, and the consequent progression in geochemical monitoring actions, during volcano evolution from dormancy to eruption.

During the repose periods of quiescent volcanoes (Fig. 9a), surface gas consists of H_2O-rich hydrothermal vapors. These WSGE emit no SO_2 and HCl, implying that ground-based remote sensing units (e.g., scanning DOAS, SO_2-camera and FTIR), and satellites, will detect no gas at all (Fig. 9a''). In this context, periodic (monthly-to-yearly) direct gas sampling of fumaroles is the most effective monitoring strategy (Fig. 9a). Any summit crater lake will also need to be sampled periodically, to test for temporal stability of temperature, salinity, and compositions. Attempts to measure the fumarolic CO_2 flux will be complicated by the absence of SO_2, and will therefore require profiling CO_2 concentrations in the plume via either ground or airborne surveys. Notably, in such closed-vent volcanoes, this fumarolic CO_2 flux (Fig. 9a'') is normally far more modest than the diffuse CO_2 output from the volcano's flank/periphery, implying that soil CO_2 monitoring is also critically important. During repose, this soil CO_2 output will be dominated by biogenic sources (soil respiration) and will likely exhibit strong seasonal modulations (Fig. 9a'').

Unrest (Fig. 9b) is typically initiated by an escalating supply of magmatic gases into the hydrologic/hydrothermal system. At this stage, the critical question is to establish if magmatic gases are supplied by decompressing (ascending) mafic magma at depth (magmatic unrest; Fig. 9c), or if instead magma is stationary and releasing volatiles due to crystallization/second boiling. In such a second case, timing and magnitude (flux) of magmatic volatile release at surface will be primarily modulated by pressure build-up underneath (and failure of) a hydrothermal seal

(hydrothermal unrest, Fig. 1c). Independent (geophysical) evidence is normally required to resolve the two scenarios, because geochemical data alone provide ambiguous results. Whatever the case, unrest can be tracked by crater fumaroles becoming hotter and more magmatic in nature, e.g., with increasing CO_2 and H_2S proportions relative to H_2O (Fig. 9b'). Fumarolic CO_2/CH_4 and CO/CO_2 ratios are also likely to increase as caused by hydrothermal conditions evolving to higher P-T because of the input of hot, oxidized magmatic fluids [12]. At this stage, it becomes increasingly convenient to combine periodic direct sampling surveys with the installation of the first continuous monitoring sensor kits, especially fully automated accumulation chambers that real-time measure the soil CO_2 flux.

If magmatic unrest progresses (Fig. 9c), and hydrothermal reactions become less and less intense, magmatic SO_2 can eventually make its way to the surface, causing the fumarolic CO_2/S_t and H_2S/SO_2 ratios to decrease (S_t is total sulfur) (Fig. 9c'), and the SO_2 flux to become detectable from ground (and eventually from satellites) (Fig. 9c''). The soil CO_2 output is also expected to increase (Fig. 9c'') due to escalating magmatic CO_2 transport, and crater lakes are anticipated to warm up, and to become increasingly acidic and saline (lakes may become permeable to gas, and eventually dry-up and disappear when eruption is approaching). As the unrest ramps up, direct sampling becomes increasingly impractical and hazardous, demanding a transition toward instrumental in-situ observations (e.g., the deployment of a fully automated Multi-GAS). Remote sensing techniques (e.g., scanning DOAS, SO_2 camera, and FTIR) also become instrumental to monitoring, with satellites becoming increasingly useful as gas and thermal output intensify.

Monitoring activity in the eruption run-up (Fig. 9d) requires careful analysis of data streamed by multi-sensor instrumental geochemical monitoring networks. High CO_2/SO_2 ratios and increasing CO_2 (and perhaps SO_2) fluxes are likely to become detectable prior (weeks to month) eruption onset (Fig. 9d' and 9d''). As the eruption starts (Fig. 9d), the operability of in-situ instruments is often compromised, demanding a combination of FTIR and airborne (drone-based) Multi-GAS measurements (for chemistry). Remote sensing techniques (from both ground and space) emerge as the key operational tool for eruption monitoring, especially to quantify the large syn-eruptive SO_2 (and HCl) fluxes (Fig. 9d').

5. Summary and future directions.

Geochemical volcano monitoring has transformed in the last few decades. By exploiting data streamed in near real-time by instrumental networks, fluid geochemistry is increasingly becoming an operational tool in the hands of volcanologists, volcanic hazard managers, and decision-makers. We have shown that capturing precursory geochemical change prior to eruption can now be achieved with increasing success when a multi-parameter, multi-instrument network is in place (Fig. 2). This network should be progressively refined as the state of the volcano evolves during unrest, making different monitoring strategies more effective, and in the run-up to eruption (Fig. 9).

We expect additional transformation in the field in the years to come, inspired by new technological development. There is growing need of increasing the number of gas species (including, for example, HCl, HF, CH_4, and CO) that can be real-time detected by in-situ permanent instruments (e.g., Multi-GAS). These instruments will need to improve in terms of robustness, operational simplicity and reduced costs, and standardized codes for near real-time data acquisition, processing, visualization, and interpretation (for example, assisted by artificial intelligence) will need to be developed, and distributed to volcano observatories worldwide. Barriers to open data sharing still exist and will need to be overcome. Drones, or UAS (unoccupied aircraft systems), have already been employed at many volcanoes for SO_2 flux measurements, Multi-GAS measurements, gas sampling, and water sampling, and more. Given drones' ability to make proximal measurements in hazardous situations and environments while operators remain at a safe distance, we expect further proliferation of innovative UAS-based volcanic gas measurements in coming years. Satellites are today primarily employed for SO_2 in geochemical volcano monitoring, but measuring other critical species for monitoring, especially CO_2, remains extremely desirable, and will potentially become a reality soon as new airborne IR sensors are deployed onboard new generations of satellites.

6. References

[2] T.A. Jr. Jaggar, Magmatic gases, American Journal of Science, 238, 5, (1940), 313–353, doi:10.2475/ ajs.238.5.313.1940.

[3] R.B. Symonds, W.I. Rose, G.J.S. Bluth, T.M. Gerlach, Volcanic-gas studies: methods, results, and applications, Rev. Mineral. Geochem. 30 (1994), 1–66.

[6] C. Oppenheimer, T.P. Fischer, B. Scaillet, Volcanic degassing, in Holland HD, Turekian KK (eds.), Treatise on Geochemistry, The Crust, 2nd edn, (2014), 111–179, Elsevier.

[7] M Edmonds, Geochemical monitoring of volcanoes and the mitigation of volcanic gas hazards, In Papale P (ed.) Hazards and Disasters Series, Forecasting and Planning for Volcanic Hazards, Risks, and Disasters, Elsevier, Volume 2, (2021) https://doi.org/10.1016/B978-0-12-818082-2.09995-9

[8] A. Aiuppa, C. Caudron, G. Chiodini, S. Ingebritsen, F. Viveiros, Geochemical monitoring of volcanic fluids in the 21st century. In Spica Z. Caudron C. (eds.) Modern Volcano Monitoring, Advances in Volcanology series, Springer Nature Switzerland AG.

[11] R. Corsaro, et al., Linking subsurface processes to surface observations - rocks, gas, deformation, seismicity (including petrology), this volume, Part 1, Chapter 5.4

[12] G. Chiodini, A. Paonita, A. Aiuppa, A. Costa, S. Caliro, P. De Martino, V. Acocella, J. Vandemeulebrouck, Magmas near the critical degassing pressure drive volcanic unrest towards a critical state, Nat. Comm., 7, (2016), 13712.

[13] O. Vaselli, F. Tassi, E. Duarte, E. Fernandez, R.J. Poreda, A.D. Huertas Evolution of fluid geochemistry at the Turrialba volcano (Costa Rica) from 1998 to

2008, Bull Volcanol 72, (2010), 397–410, https:// doi. org/ 10. 1007/ s00445- 009-0332-4.

[14] Y. Taran, M. Zelenski, Systematics of water isotopic composition and chlorine content in arc-volcanic gases, Geol Soc Spec Publ, 410 (1), (2015), 237-262, DOI: 10.1144/SP410.5

[15] R.B. Symonds, T.M. Gerlach, M. H. Reed, Magmatic gas scrubbing: implications for volcano monitoring, J. Volcanol. Geotherm. Res., 108, (2001), 303–341

[16] M. Agusto, MC. Lamberti, F. Tassi, et al. Eleven-year survey of the magmatic-hydrothermal fluids from Peteroa volcano: identifying precursory signals of the 2018-2019 eruption, Geochemistry, Geophysics, Geosystems, 24-11, (2023), https://doi.org/10.1029/2023GC011064

[17] G.V. Melián, P.A. Hernández, N.M. Pérez, et al., Insights from Fumarole Gas Geochemistry on the Recent Volcanic Unrest of Pico do Fogo, Cape Verde Frontiers in Earth Science, 9, 631190, (2021), doi: 10.3389/feart.2021.631190

[18] J.M. de Moor, et al, Turmoil at Turrialba Volcano (Costa Rica): Degassing and eruptive processes inferred from high-frequency gas monitoring, J Geophys Res: Solid Earth, 121 (8), (2016), 5761-5775, DOI: 10.1002/2016JB013150.

[18] P. Allard, M. Burton, F. Muré, Spectroscopic evidence for a lava fountain driven by previously accumulated magmatic gas, Nature 433, (2005) ,407–410.

[19] S. Hidalgo, J. Battaglia, S. Arellano, et al., Evolution of the 2015 Cotopaxi eruption revealed by combined geochemical and seismic observations. Geochemistry, Geophysics, Geosystems, 19, (2018), 2087–2108. https://doi.org/10.1029/2018GC007514

[20] M. Patrick, T. Orr, D. Swanson, B. Houghton, K. Wooten, L. Desmither, C. Parcheta, D. Fee, Kīlauea's 2008–2018 summit lava lake—Chronology and eruption insights, In Patrick, M., Orr, T., Swanson, D., and Houghton, B., eds., The 2008–2018 summit lava lake at Kīlauea Volcano, Hawai'i: U.S. Geological Survey Professional Paper 1867, (2021), https://doi.org/10.3133/pp1867A.

[21] S.A. Carn, L. Clarisse, A.J. Prata, Multi-decadal satellite measurements of global volcanic degassing Journal of Volcanology and Geothermal Research, 311, (2016), 99-134. DOI: 10.1016/j.jvolgeores.2016.01.002

[22] Surono et al., The 2010 explosive eruption of Java's Merapi volcano—A '100-year' event, Journal of Volcanology and Geothermal Research, 241–242, (2012) 121-135, https://doi.org/10.1016/j.jvolgeores.2012.06.018

[23] G. Chiodini, R. Cioni, M. Guidi, B. Raco, L. Marini, Soil CO_2 flux measurements in volcanic and geothermal areas, Applied Geochemistry, 13 (5), (1998), 543-552. DOI: 10.1016/S0883-2927(97)00076-0

[24] S. Inguaggiato, F. Vita, M. Cangemi, C. Inguaggiato, L. Calderone, The monitoring of CO_2 soil degassing as indicator of increasing volcanic activity: The paroxysmal activity at Stromboli volcano in 2019–2021. Geosciences, 11(4), (2021), 169.

[25] G. Melián, P.A. Hernández, E. Padrón, N.M. Pérez, J. Barrancos, G. Padilla, S. Dionis, F. Rodríguez, D. Calvo, and D. Nolasco, Spatial and temporal variations of diffuse CO2 degassing at El Hierro volcanic system: Relation to the 2011–2012 submarine eruption, J. Geophys. Res. Solid Earth, 119, (2014), 6976–6991, doi:10.1002/2014JB01101

7. References to other EoV chapters

[1] J. Stix, P. Nadeau, F. Aguilera, M. Burton, A. Chiodi. Volcanic degassing, this volume, Part 3, Chapter 2.8

[4] M. Edmonds, A-S Bouvier, E. Hughes, K. Iacovino, K. Roggensack, A. Shahar, Origins of magmatic volatiles and their role in magma ascent and degassing, this volume, Part 1, Chapter 2.2

[5] T.P. Fischer, G. Chiodini, Volcanic, magmatic and hydrothermal gases. In Sigurdsson, H., editor, The Encyclopedia of Volcanoes, 2nd edition, chapter 45 (2015), 779–797, Academic Press, Amsterdam.

[9] P. Delmelle, J. Stix, Volcanic gases, In: Encyclopedia of Volcanoes, Sigurdsson H (ed) Academic Press, San Diego, (2000), 803-815

[10] J. Stix, H. Gaonach, Gas, plume and thermal monitoring, In Encyclopædia of volcanoes. Edited by Sigurdsson H., Academic Press, (2000), 1141–1164.

[26] P. Delmelle, R.W. Henley, A. Bernard, Volcano-Related Lakes, In Sigurdsson, H., editor, The Encyclopedia of Volcanoes, 2nd edition, chapter 45 (2015), 851–864, Academic Press, Amsterdam.

[27] H. Shinohara, C. Finn, P. Delmelle, M. Heap, J. Hedenquist, D. Rouwet, B. Scheu, V. Van Hinsberg, Acid altered terrains: Formation, hazards and related uses, this volume, Part 8, Chapter 3.3

8. Further readings

Aiuppa, A. (2009), Degassing of halogens from basaltic volcanism: Insights from volcanic gas observations Chemical Geology, 263 (1-4), 99-109. DOI: 10.1016/j.chemgeo.2008.08.022

A. Aiuppa, Y. Moussallam, Hydrogen and hydrogen sulphide in volcanic gases: abundance, processes, and atmospheric fluxes, Comptes Rendus - Geoscience, 356, (2023), 1-24, DOI: 10.5802/crgeos.235

Aiuppa A, Federico C, Giudice G, Gurrieri S (2005) Chemical mapping of a fumarolic field: La Fossa Crater, Vulcano Island (Aeolian Islands, Italy). Geophys Res Lett 32 (13):1–4. http://dx.doi.org/10.1029/2005GL023207http://dx.doi.org/10.1029/2005GL023207

Aiuppa, A., Fischer, T. P., Plank, T., and Bani, P. (2019). CO2 flux emissions from the Earth's most actively degassing volcanoes, 2005–2015. Scientific Reports, 9, 5442. https://doi.org/10.1038/s41598-019-41901-y

911 Arellano, S., Galle, B., Apaza, F., Avard, G., Barrington, C., Bobrowski, N.,
912 Bucarey, C., Burbano, V., Burton, M., Chacón, Z., Chigna, G., Clarito, C. J., Conde,
913 V., Costa, F., De Moor, M., Delgado-Granados, H., Di Muro, A., Fernandez, D.,
914 Garzón, G., Gunawan, H., Haerani, N., Hansteen, T. H., Hidalgo, S., Inguaggiato,
915 S., Johansson, M., Kern, C., Kihlman, M., Kowalski, P., Masias, P., Montalvo, F.,
916 Möller, J., Platt, U., Rivera, C., Saballos, A., Salerno, G., Taisne, B., Vásconez, F.,
917 Velásquez, G., Vita, F., and Yalire, M.: Synoptic analysis of a decade of daily
918 measurements of SO2 emission in the troposphere from volcanoes of the global
919 ground-based Network for Observation of Volcanic and Atmospheric Change,
920 Earth Syst. Sci. Data, 13, 1167–1188, https://doi.org/10.5194/essd-13-1167-2021,
921 2021.

922 Bobrowski N, Honninger G, Galle B, and Platt U (2003) Detection of bromine
923 monoxide in a volcanic plume. Nature 423: 273–276.

924 Burton M, Allard P, La Spina A, Murè F (2007) Magmatic gas composition reveals
925 the source depth of slug-driven strombolian explosive activity. Science 317: 227–
926 230. Doi:10.1126/science.1141900.

927 Carn, S. A., Fioletov, V. E., McLinden, C. A., Li, C., and Krotkov, N. A. (2017). A
928 decade of global volcanic SO2 emissions measured from space. Scientific
929 Reports, 7, 44095. https://doi.org/10.1038/srep44095

930 Chiodini, G., R. Cioni and L. Marini (1993) Reactions governing the chemistry of
931 crater fumaroles from Vulcano Island, Italy, and implications for volcanic
932 surveillance. Appl. Geochem. 8, 357–371. http://dx.doi.org/10.1016/0883-
933 2927(93)90004-Z.

934 Christenson B, Németh K, Rouwet D, Tassi F, Vandemeulebrouck J, Varekamp
935 JC (2015) Volcanic lakes. In Volcanic lakes. Springer, Berlin, p 1–20.

936 de Moor, J.M., Fischer, T.P., Sharp, Z.D., King, P.L., Wilke, M., Botcharnikov, R.E.,
937 Cottrell, E., Zelenski, M., Marty, B., Klimm, K., Rivard, C., Ayalew, D., Ramirez, C.
938 (2013) Sulfur degassing at Erta Ale (Ethiopia) and Masaya (Nicaragua):
939 Implications for degassing processes and oxygen fugacities of basaltic systems.
940 Geochem. Geophys. Geosyst. https://doi.org/10.1002/ggge.20255.

941 Edmonds M, Liu EJ, Cashman KV (2022) Open-vent volcanoes fuelled by depth-
942 integrated magma degassing. Bull Volcanol 84:28 https://doi.org/10.1007/s00445-
943 021-01522-8.

944 Edmonds M, Wallace PJ (2017) Volatiles and Exsolved Vapor in Volcanic
945 Systems. Elements 13: 29–34

946 Fischer, T. P., and A. Aiuppa (2020). AGU Centennial Grand Challenge:
947 Volcanoes and deep carbon global CO2 emissions from subaerial volcanism—
948 Recent progress and future challenges. Geochemistry, Geophysics, Geosystems,
949 21, e2019GC008690. https://doi.org/10.1029/2019GC008690

Fournier, R. O. (1999) Hydrothermal processes related to movement of fluid from plastic into brittle rock in the magmatic-epithermal environment. Econom. Geol. 94, 1193–1211

Francis P, Burton MR, Oppenheimer C (1998) Remote measurements of volcanic gas compositions by solar occultation spectroscopy. Nature 396: 567–570.

G. Chiodini, L. Marini, Hydrothermal gas equilibria: The H2O-H2-CO2-CO-CH4 system Geochimica et Cosmochimica Acta, 62 (15), (1998), 2673-2687.DOI: 10.1016/S0016-7037(98)00181-1

Giggenbach W. F. and Goguel R. L. (1989) Collection and analysis of geothermal and volcanic water and gas discharges. DSIR Chemistry, Rept. No. 2401

Gutmann, A., Bobrowski, N., Liotta, M., Hoffmann, T. (2021) Bromine speciation in volcanic plumes: New in situ derivatization LC-MS method for the determination of gaseous hydrogen bromide by gas diffusion denuder sampling. Atmospheric Measurement Techniques, 14 (10), pp. 6395-6406. DOI: 10.5194/amt-14-6395-2021

Kern, C., P. Masias, F. Apaza, K. A. Reath, and U. Platt (2017), Remote measurement of high preeruptive water vapor emissions at Sabancaya volcano by passive differential optical absorption spectroscopy, J. Geophys. Res. Solid Earth, 122, 3540–3564, doi:10.1002/2017JB014020

Mori T and Burton M (2006) The SO2 camera: A simple, fast and cheap method for ground-based imaging of SO2 in volcanic plumes. Geophysical Research Letters 33: L24804.

Oppenheimer, C., B. Scaillet, R.S. Martin (2011) Sulfur degassing from volcanoes: source conditions, surveillance, plume chemistry and earth system impacts Reviews in mineralogy and geochemistry 73 (1), 363-421

Pasternack G.B., J.C. Varekamp, (1997) Volcanic lake systematics. I.: physical constraints, Bull. Volcanol. 58, 528–538.

Rouwet D, Tassi F, Mora-Amador R, Sandri L, Chiarini V (2014) Past, present and future of volcanic lake monitoring. J Volcanol Geotherm Res 272: 78-97. https://doi.org/10.1016/j.jvolgeores.2013.12.009.

Rüdiger, J., Gutmann, A., Bobrowski, N., Liotta, M., de Moor, J. M., Sander, R., Dinger, F., Tirpitz, J.-L., Ibarra, M., Saballos, A., Martínez, M., Mendoza, E., Ferrufino, A., Stix, J., Valdés, J., Castro, J. M., and Hoffmann, T.: (2021) Halogen activation in the plume of Masaya volcano: field observations and box model investigations, Atmos. Chem. Phys., 21, 3371–3393, https://doi.org/10.5194/acp-21-3371-2021

Scott, S., A. Seward, G. Ryan, E. Joseph, S. Hurwitz, P. Utami, C. Munoz-Saez, F. Samrock, W. Cumming, I. Chambefort. Mining heat from geothermal systems in volcanic terrain. this volume, Part 8, Chapter 3.1

Shinohara H (2005) A new technique to estimate volcanic gas composition: plume measurements with a portable multi-sensor system. J Volcanol Geotherm Res 143,319–333

Symonds, R.B., Gerlach, T.M., Reed, M.H. (2001) Magmatic gas scrubbing: implications for volcano monitoring. J Volcanol Geotherm Res 108:303–341. https:// doi.org/ 10.1016/ S0377- 0273(00) 00292-4

Varekamp JC (2015) The Chemical Composition and Evolution of Volcanic Lakes. In Rouwet D, Christenson B, Tassi F, Vandemeulebrouck J (eds.), Volcanic Lakes, p. 93-123. Advances in Volcanology. Berlin, Heidelberg: Springer. https://doi.org/10.1007/978-3-642-36833-2_4

Werner, C., W.C. Evans, P. Kelly, McGimsey, M.A. Pfeffer, M.P. Doukas, T. Neal (2012) Deep magmatic degassing vs. scrubbing: elevated CO_2 and C/S ratios in the lead-up to the 2009 eruption of Redoubt Volcano, Alaska. Geochemistry, Geophysics, Geosystems 13 (1), http://dx.doi.org/10.1029/2011GC003794.

9. Figure and figure captions.

Figure 1 – A) A schematic cross-section of a SVGE (Strong Volcanic Gas Emitters) volcano. The magmatic gases they release (by either open-vent degassing or hot dome-hosted fumaroles) are H_2O-CO_2-SO_2 mixtures. In the triangular plot of panel B), these magmatic gases are exemplified by the yellow (data from a global database) and red (Etna) circles. At any given volcano, gas compositional change is controlled by changes in magma degassing depth and extent; see the Etna example (red circles are selected plume results from the Bocca Nuova crater, which range from CO_2-rich deeply exsolved gas to SO_2-rich shallow sourced gas). C) A schematic cross-section of a WVGE (Weak Volcanic Gas Emitters) volcano. Gases are H_2O-CO_2-H_2S mixtures formed by boiling of meteoric water-dominated hydrothermal aquifers, heated by magmatic gases released by magma stored at depth. A hydrothermal mineral seal separates the ductile and brittle crust and modulates (via press-build-up until failure) the rate of magmatic gas supply. At these WVGE volcanoes, the main drivers of chemical change are temporally variable extents of (i) mixing between magmatic and hydrothermal gases, (ii) sulfur scrubbing in (or remobilization from) hydrothermal minerals/fluids, (iii) steam/condensation, and (iv) meteoric water addition. Hydrothermal to magmatic gas transition is exemplified by the Turrialba gas dataset [13]; D) Relative proportions of C species. Hydrothermal gases from WVGE are CH_4-enriched, and are interpreted to reflect equilibration in the liquid (L), vapor (V) or superheated vapor (SHV) over a range of hydrothermal temperatures (light blue dashed °C). Drivers of change (as exemplified by the Campi Flegrei case) are either changing hydrothermal P-T-X conditions, or mixing with magmatic gases, that are CO-rich and CH_4-poor (often CH_4-free; data from [5]).

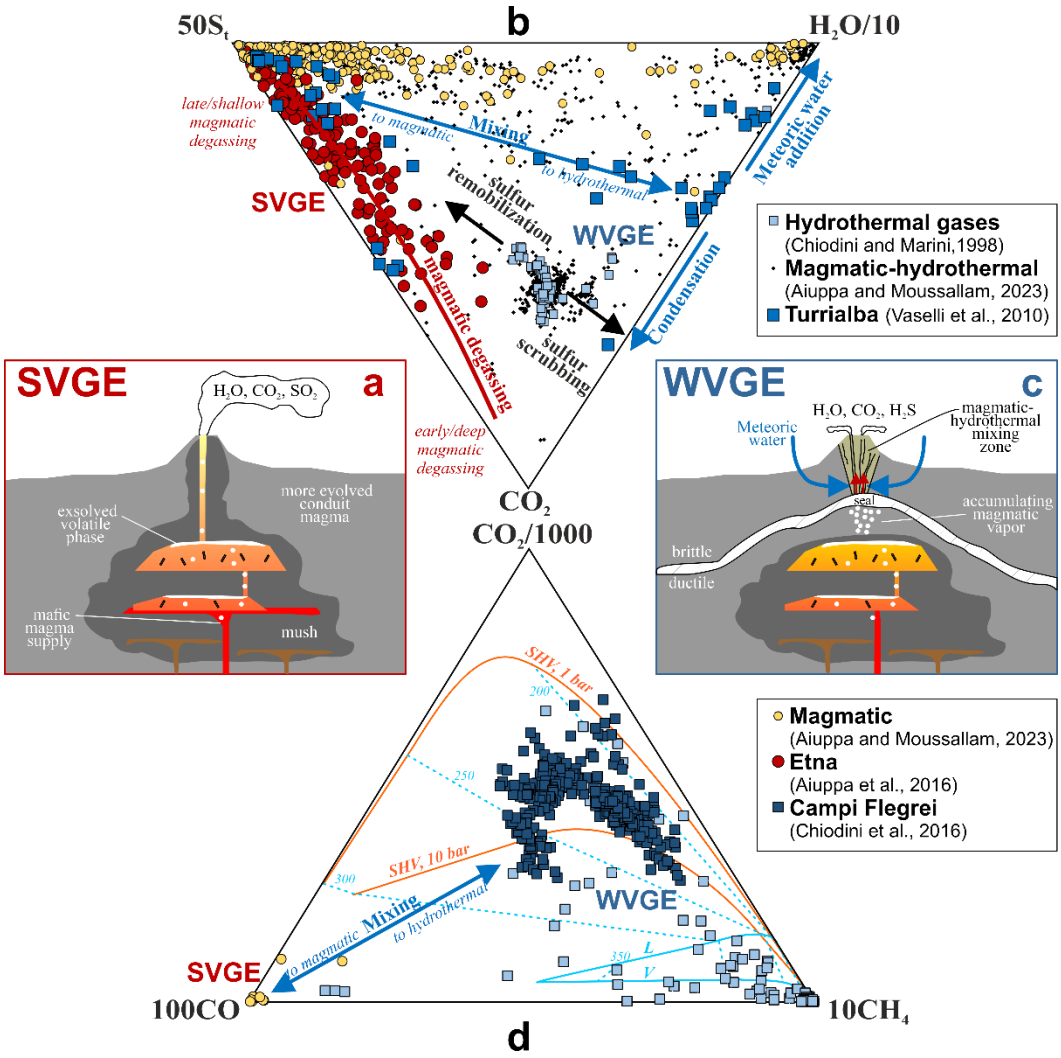
b
50S$_t$
H$_2$O/10
CO$_2$
CO$_2$/1000
late/shallow magmatic degassing
to magmatic
Mixing
to hydrothermal
Meteoric water addition
SVGE
Sulfur remobilization
WVGE
magmatic degassing
Condensation
Sulfur scrubbing
early/deep magmatic degassing
Hydrothermal gases
(Chiodini and Marini,1998)
Magmatic-hydrothermal
(Aiuppa and Moussallam, 2023)
Turrialba (Vaselli et al., 2010)
SVGE
a
H$_2$O, CO$_2$, SO$_2$
more evolved conduit magma
exsolved volatile phase
mafic magma supply
mush
WVGE
c
H$_2$O, CO$_2$, H$_2$S
Meteoric water
magmatic-hydrothermal mixing zone
Seal
accumulating magmatic vapor
brittle
ductile
SHV, 1 bar
200
250
SHV, 10 bar
300
Mixing
to magmatic
to hydrothermal
WVGE
350
L
V
SVGE
100CO
10CH$_4$
Magmatic
(Aiuppa and Moussallam, 2023)
Etna
(Aiuppa et al., 2016)
Campi Flegrei
(Chiodini et al., 2016)
d

1030

1031

Figure 2 – Integrated geochemical monitoring network during A) repose, B) escalating degassing (unrest), C) eruption. Turrialba volcano in background (photo credits, J.M.D.M).

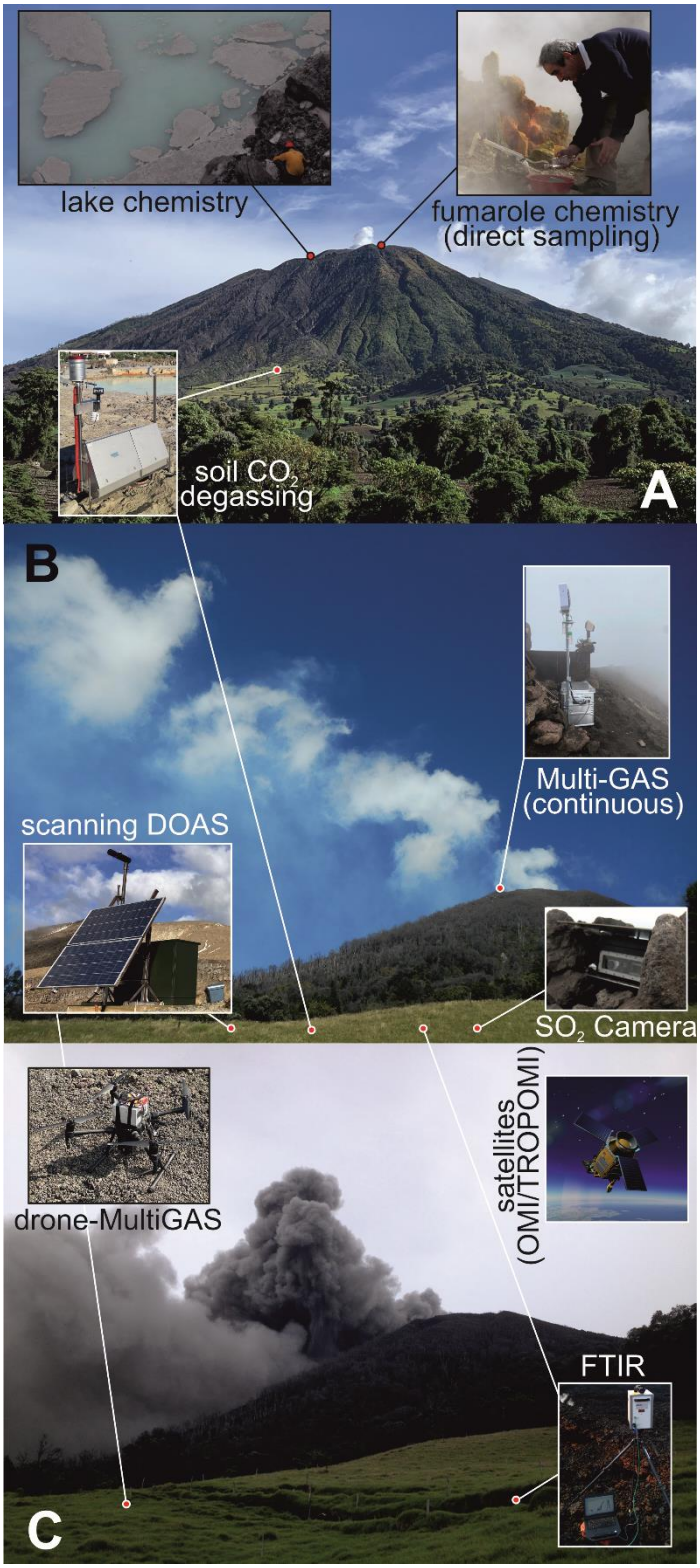

Figure 3 - a) Peteroa volcano gas time series. The panels illustrate the temporal evolution (2010 to 2021) of SO_2/H_2S, 100*HCl/CO_2, 1000*HF/CO_2 (thin dashed lines point out 0.1 ratio values), CH_4/Ar ratios, $^3He/^4He$ (Rc/Ra), and $\delta^{13}C\text{-}CO_2$ (‰vs. V-PDB) in fumarolic gases [16]. b) Pico do Fogo volcano gas time series. The plot illustrates the temporal evolution (2007 to 2018) of CO/CO_2, H_2/CO_2, $\delta^{13}C\text{-}CO_2$ (‰vs. V-PDB), and equilibrium temperature (EqT; estimated based on the $CH_4\text{-}CO\text{-}CO_2$ system: $3CO_2 + CH_4 \Leftrightarrow 4CO + 2H_2O$) in two fumarolic vents (F1 and F2) [17]. Gray shaded areas highlight phases with magmatic gas signatures. The phreatic, phreato-magmatic, and magmatic eruptions (between thick dashed lines) are also indicated.

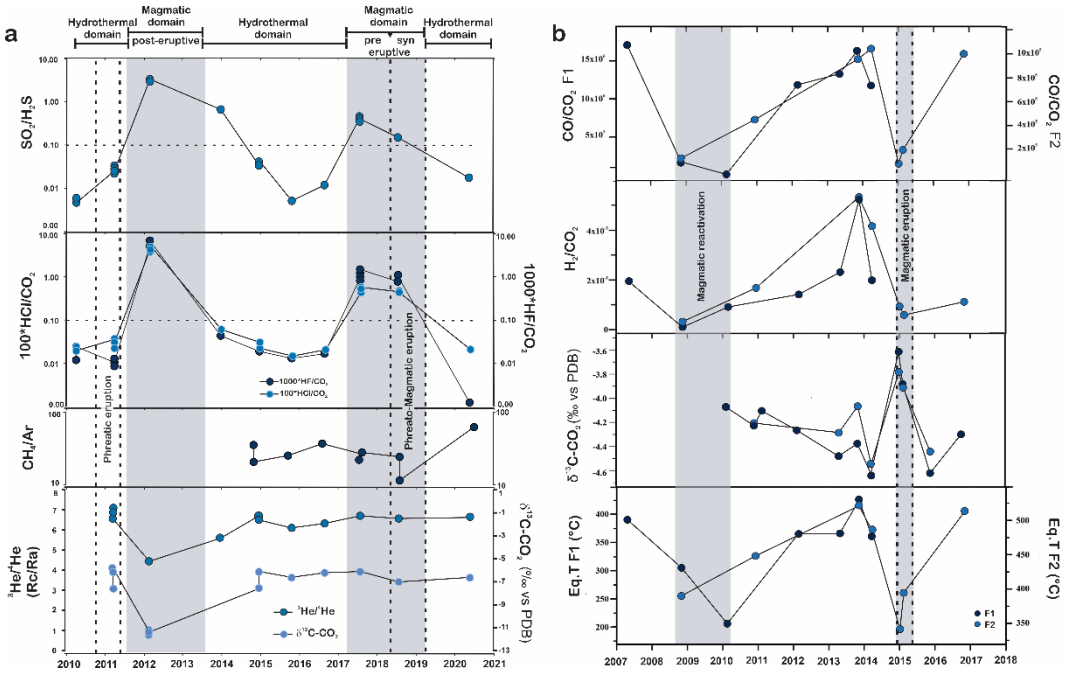

Figure 4 - Changes in gas compositions at Turrialba volcano from direct sampling (left panels, 1998-2008) and Multi-GAS (right panels, 2014-2020) tracked the displacement of the hydrothermal system by magma intrusion, preceding vent-opening eruptions, years of semi-continuous ash emissions, and small Strombolian eruptions (note a small Multi-GAS data gap in 2019).

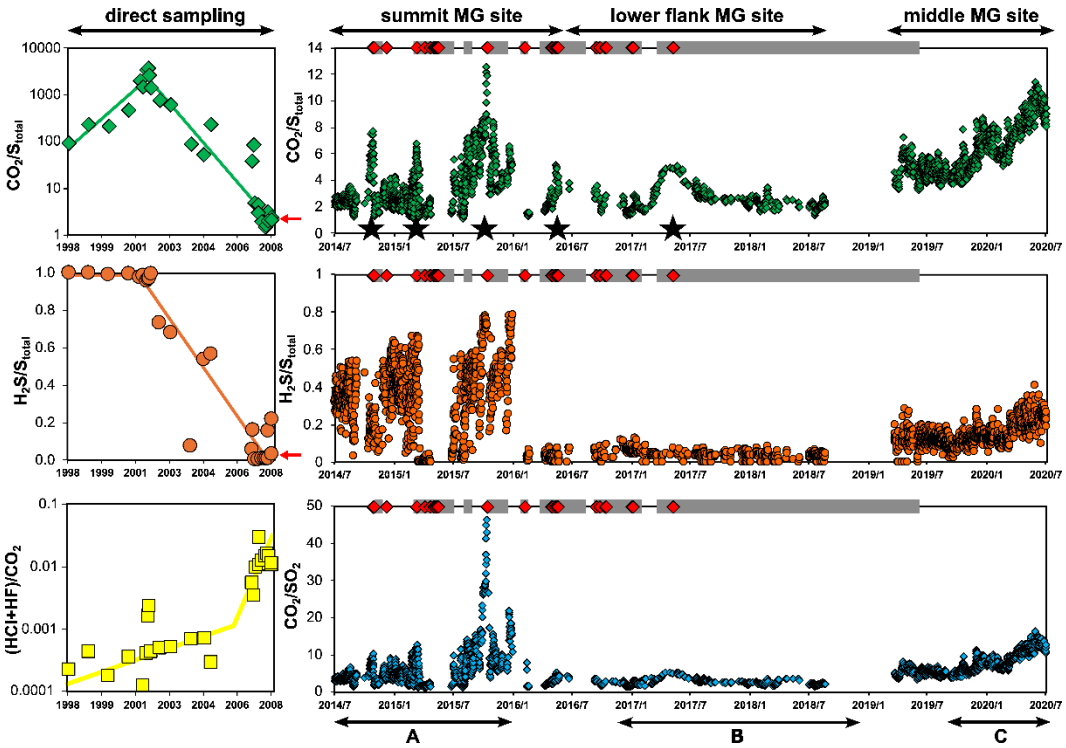

Figure 5 - Top: SO_2 emissions (red), transient seismic events per day (gray), and SO_2/HCl ratios (blue) during 2015 at Cotopaxi Volcano. Both seismicity and SO_2 emissions began to increase months in advance of the eventual eruptive activity in mid-August, indicating shallowing magma. The detection of HCl in early August further supported the interpretation that magma was nearing the surface. Seismic data courtesy of Silvana Hidalgo. Gas data available at http://dx.doi.org/10.1594/IEDA/111165. Bottom: SO_2 emissions (red), weekly RSAM (station RIM, gray), and GPS North-South displacement (station UWEV, blue) in late 2007 and early 2008 at the summit of Kīlauea. Though GPS indicated continued shallow deflation, both seismic tremor and SO_2 emissions began to climb above background in November and December of 2007, hinting at shallowing magma. A new fumarole field appeared on 12 March 2008 and became incandescent a few days later, less than a week before the onset of the new eruption. Data from ref. [20] references therein.

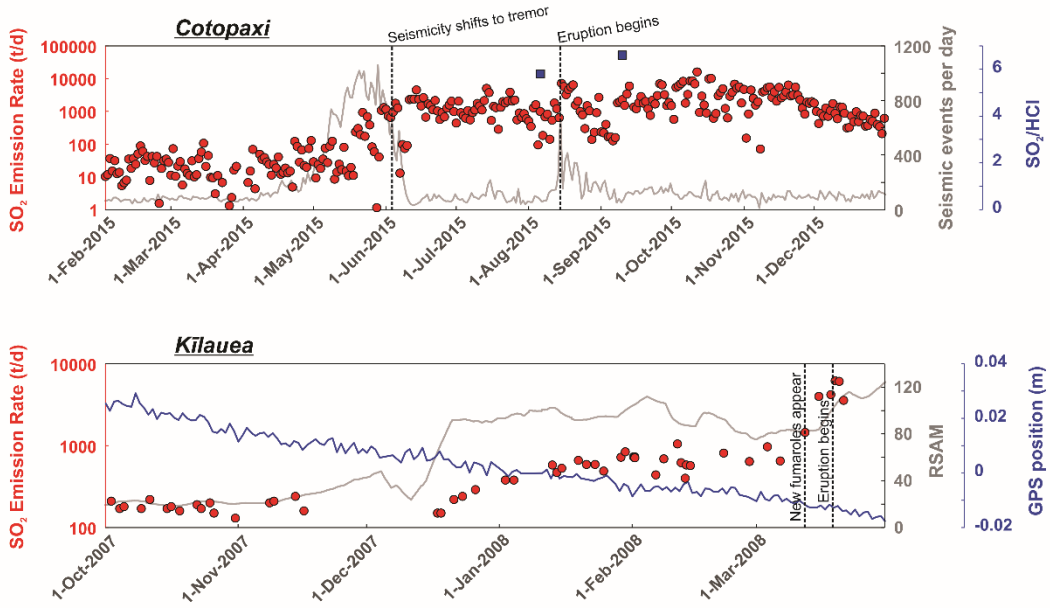

Figure 6 - Time series of annual mean SO_2 emissions in 2005-2022 for 104 degassing volcanoes derived from NASA/Aura Ozone Monitoring Instrument (OMI) satellite observations. Each panel shows the SO_2 time series for the indicated volcano (white or gray curve) on a log scale (y-axis is scaled from 0.01-20 kilotons/day on each plot), the mean SO_2 flux (*horizontal red line*), and the SO_2 flux (kt/day) in 2022 (red dot; only shown if >0.01 kt/day). Panels are colored and ordered based on the percentage difference between the SO_2 flux in 2022 and the mean SO_2 flux.

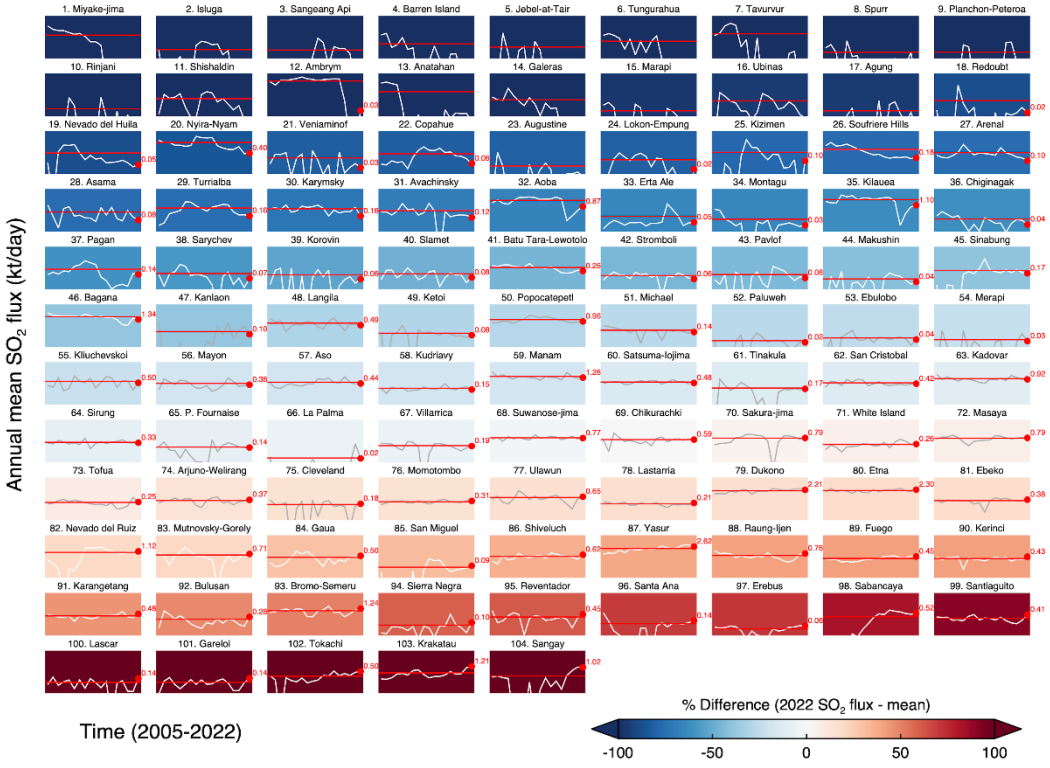

1081

1082

Figure 7- a) Daily averaged (24 measurements/day) CO_2 fluxes at Stromboli in the 2001 to 2018 period. Onset of the 2002–2003, 2007, 2014, and 2019 eruptions are indicated. B) Sketch of the stromboli plumbing system: exsolved volatiles from the degassing magma are primarily emitted by the plume, and partially interact with a summit hydrothermal system to feed cold fumaroles, diffuse soil degassing, and thermal waters. When the dynamic equilibrium between gas input and output is altered by increasing magmatic gas supply from depth, the hydrothermal system releases more CO_2 to the surface; C) Time series of the 24 h moving averages of diffuse CO_2 flux at a fixed station (gray) and temporal evolution of total diffuse CO_2 flux (black) during 2011–2012 at El Hierro volcano. Time is expressed in days before/after eruption onset.

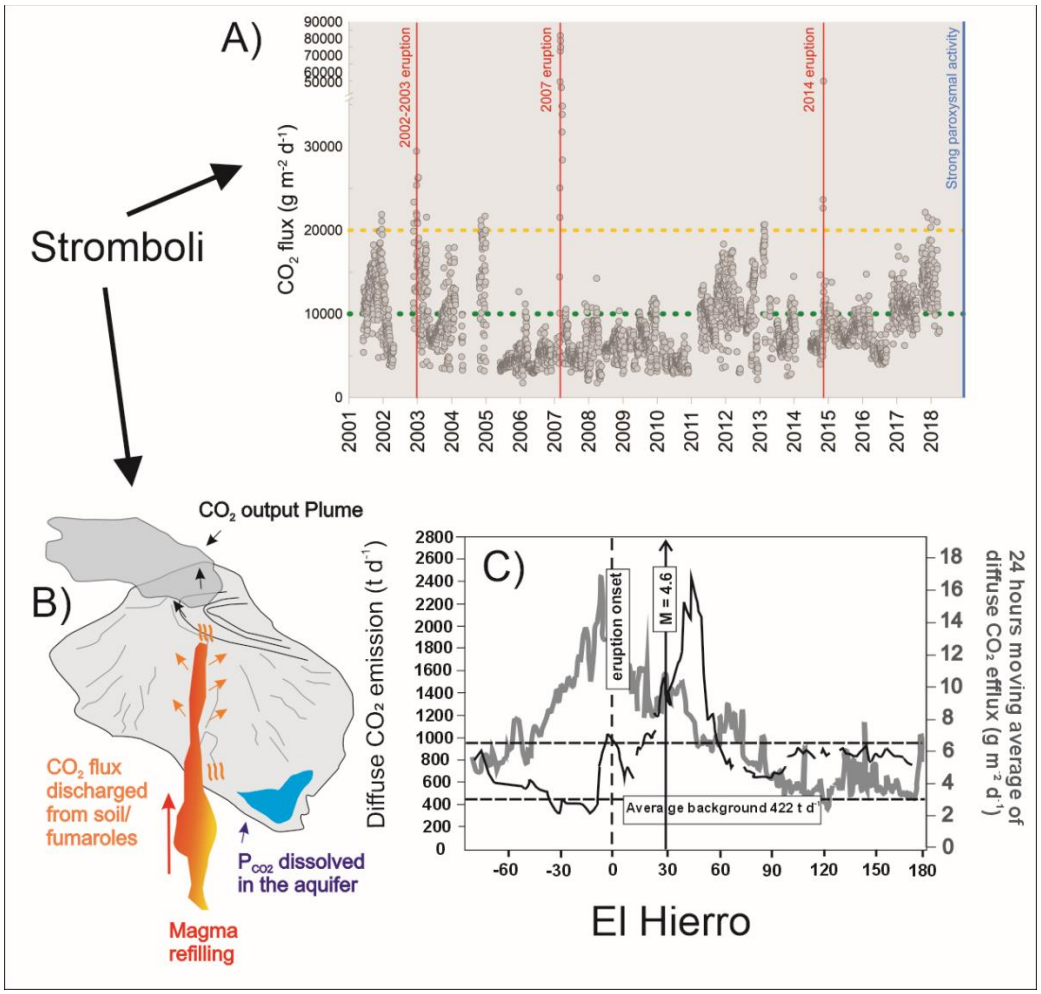

Figure 8: (right) Sketch showing the typical structure of a hyper-acid high-activity lake. (Left) Idealized time series illustrate the expected changes for a few key geochemical monitoring parameters for 2 end-member cases: Red lines show the expected progression for the run-up to an eruption driven by deep magma injection and magma rising to the surface, whereas the blue lines show the expected progression for a system that becomes hydrothermally sealed and then erupts due to pressure/volatile accumulation below the seal. The process leading up to eruption starts at t_1, where new magma starts being injected, raising lake temperature (until the lake evaporates at t_3). Fresh rock in the system drives Mg/Cl up, rising magma drives increasing SO_2 degassing (which increases further once the lake disappears at t_3), initially associated with an increase in CO_2/SO_2 (deep magma recharge initiating the process) and then decreasing CO_2/SO_2 as the magma rises (another drop in CO_2/SO_2 occurs at the time of the eruption as magma remobilizes S from the sublimnic alteration zone). For the case of pressure accumulation by sealing, the lake temperature decreases, then surges once the eruption breaks the seal, and then the lake evaporates completely. Mg/Cl stays constant until the seal breaks, which releases deeper Mg-rich fluids, and Mg/Cl increases as the lake evaporates. SO_2 flux decreases as sealing occurs, then comes out moderately as the accumulated SO_2 is released. CO_2/SO_2 increases with sealing, then drops to shallow magmatic values as the seal breaks, and then goes back to background values.

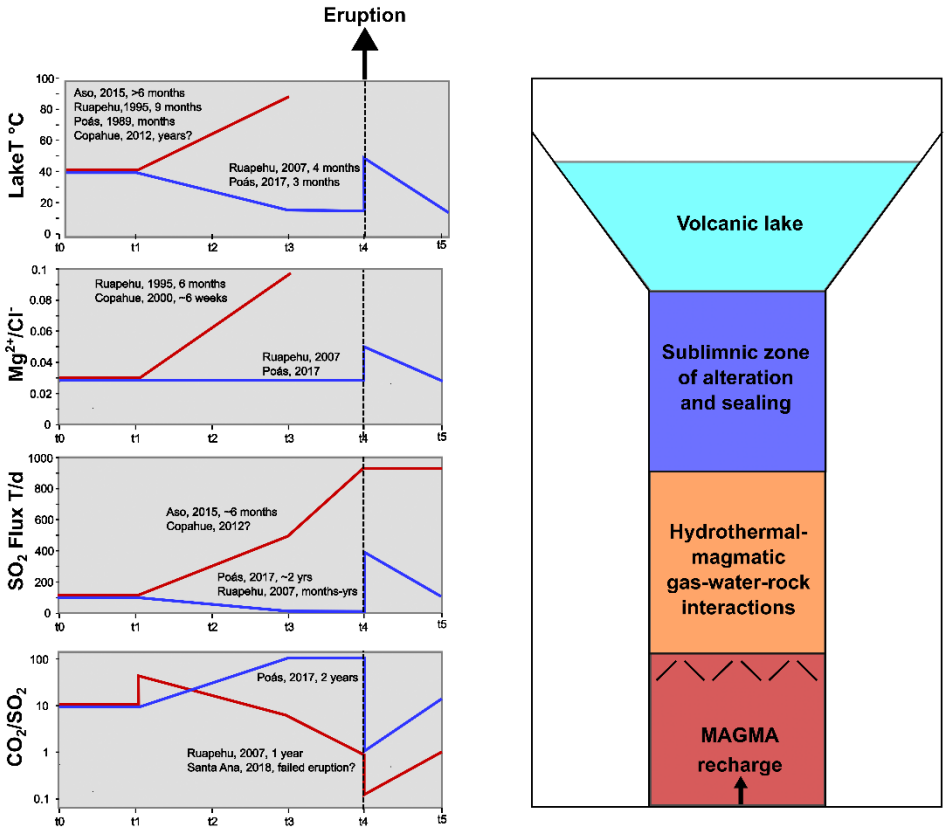

1117

Figure 9 - A schematic, purely illustrative model describing the expected sequence of geochemical changes (panels A' to D'') during a hypothetical volcano dormancy-to-eruption progression. Panels A to D exemplify key processes in the magmatic plumbing system and in the overlying hydrothermal system. The two are thought to be separated by a hydrothermal mineral seal at which the ductile-brittle transition occurs (note the ductile brittle transition is here exemplified as a layer, but rather correspond to progressive, dynamic (in space and time) transitional environment from ductile rocks to brittle rocks and therefore a permeability transition). Seismicity (stars) and deformation (dashed line + arrows) patterns are also schematically illustrated. Time is in arbitrary units, and the chemical changes are purely hypothetical and for illustration purposes only. A recommended progression of geochemical monitoring actions is illustrated in the top panels. A continuous instrumental monitoring network is critically demanded to capture short-term changes prior to eruption, and to follow/monitor ongoing eruptions. This network should also ideally be in place at any SVGE (at both mafic open-vent volcanoes and more silicic dome-hosting volcanoes).